

## ORIGINAL RESEARCH ARTICLE

# Ellagic acid from *Terminalia leiocarpa* downregulates estrogen-dependent signaling and epithelial-to-mesenchymal transition canonical pathways in MCF-7 cells

**Temitope O. Lawal<sup>1</sup>**, **Pinal N. Kanabar<sup>2</sup>**, **Nina S. Los<sup>3</sup>**, **Shitalben M. Patel<sup>1</sup>**, **Mark Maienschein-Cline<sup>2</sup>**, **Zarema H. Arbieva<sup>3</sup>**, **Bolanle A. Adeniyi<sup>1</sup>**, and **Gail B. Mahady<sup>1\*</sup>**

<sup>1</sup>Department of Pharmacy Practice, Retzky College of Pharmacy, World Health Organization Collaborating Centre for Traditional Medicine, University of Illinois Chicago, Chicago, Illinois, United States of America

<sup>2</sup>Research Informatics Core, Research Resources Center, University of Illinois Chicago, Chicago, Illinois, United States of America

<sup>3</sup>Genomics Research Core, Research Resources Center, University of Illinois Chicago, Chicago, Illinois, United States of America

### \*Corresponding author:

Gail B. Mahady  
(mahady@uic.edu)

**Citation:** Lawal TO, Kanabar PN, Los NS, *et al.* Ellagic acid from *Terminalia leiocarpa* downregulates estrogen-dependent signaling and epithelial-to-mesenchymal transition canonical pathways in MCF-7 cells. *Innov Med Omics*. 2026;3(2):025470062. doi: 10.36922/IMO025470062

**Received:** November 19, 2025

**Revised:** January 14, 2026

**Accepted:** January 21, 2026

**Published online:** April 7, 2026

**Copyright:** © 2026 Author(s). This is an Open-Access article distributed under the terms of the Creative Commons Attribution License, permitting distribution, and reproduction in any medium, provided the original work is properly cited.

**Publisher's Note:** AccScience Publishing remains neutral with regard to jurisdictional claims in published maps and institutional affiliations.

## Abstract

Breast cancer remains the most diagnosed cancer among women worldwide, and its prevalence continues to increase annually. Previously, we reported that ellagic acid (EA), a compound isolated from *Terminalia leiocarpa* (DC.) Baill., a plant used in Nigerian traditional medicine, inhibited the proliferation of cultured human MCF-7 breast cancer cells. EA is a pharmacologically active polyphenolic compound with antioxidant, anti-inflammatory, and anti-estrogenic activities. In this work, we investigated the effects of EA on the transcriptome of MCF-7 cells using next-generation sequencing. After EA treatment, MCF-7 cells were harvested, and total RNA was isolated and used to prepare RNA sequencing libraries. Sequencing was performed using NovaSeq 6000. The results showed that EA significantly altered gene expression patterns in MCF-7 cells. Bioinformatic analysis of the sequencing data revealed that 4,848 transcripts were differentially expressed, with 2,180 upregulated genes and 2,668 downregulated genes ( $q \leq 0.01$ ). Ingenuity Pathway Analysis indicated that EA-induced expression changes mapped to 98 canonical pathways, including upregulation of apoptosis signaling pathways and downregulation of estrogen signaling and estrogen-dependent breast cancer signaling pathways ( $q \leq 0.05$ ). Furthermore, EA downregulated gene expression in the epithelial-to-mesenchymal transition (EMT) canonical pathway, such as *PRRX1/2*, *TGF*, *TWIST1*, and *VIM*. These data indicate that EA has multiple mechanisms of action in MCF-7 cells, including the induction of apoptosis and the reduction of both estrogen and EMT signaling. Thus, with further research, EA may serve as an inexpensive, safe, and effective treatment for breast cancer and metastatic diseases.

**Keywords:** Apoptosis; Breast cancer; Deep sequencing; Epithelial-to-mesenchymal transition; Estrogen receptor; Transcriptomics

## 1. Introduction

Breast cancer (BC) is currently the most common form of cancer among women worldwide, with occurrences in every country.<sup>1</sup> According to a 2022 World Health Organization global report, BC was the most diagnosed cancer in women in 157 of 185 countries, with ~2.3 million new cases and ~670,000 deaths due to complications of the disease.<sup>1</sup> In Africa, the incidence of BC is lower than in other continents (except Asia); however, the prevalence continues to increase, and Africa has the highest age-standardized mortality rate for BC among continents.<sup>2–5</sup> BC-related mortality rates are highest in the northern and western countries of Africa, at ~24.7% and 27.1%, respectively.<sup>4</sup> Nigeria in West Africa has a BC prevalence rate of 69.1 per 100,000 and a high mortality rate of 25.5 per 100,000 people.<sup>2,3</sup> BC-related deaths are lower in Central and Eastern Africa at 23.9% and 17.9%, respectively, and the lowest death rates are observed in South African countries (15%).<sup>4</sup>

One scoping review and meta-analysis of BC phenotypes in Africa reported that the frequencies of hormone receptor-positive (HR+; luminal), human epidermal growth factor receptor 2-positive (HER2+), and triple-negative BCs were ~56.30%, 12.61%, and 28.10%, respectively.<sup>4</sup> The study also reported that the highest level of the HR+ subtype was observed in North Africa, while HER2+ and triple-negative BCs were more frequent in West Africa.<sup>4</sup> Thus, as in the United States, HR+ BCs (luminal A and B molecular subtypes) are the most common BCs in Africa.<sup>1,4</sup>

While Western medicines are widely available in Nigeria, plant-based medicines and traditional medicine practices are still commonly used by ~70% of the population.<sup>6,7</sup> Many of these medicinal plants have been reported to treat various diseases, including infections and cancer, but often have little scientific evidence to support their use.<sup>8</sup> One such plant, *Terminalia leiocarpa* (DC.) Baill. (syn. *Anogeissus leiocarpus* [DC.] Guill. & Perr.) (Combretaceae) is a deciduous tree, endemic to West and East Africa, and commonly referred to as African birch.<sup>9–11</sup> While much of the published literature refers to the plant as *Anogeissus leiocarpus*, *Terminalia leiocarpa* is now the accepted genus and species according to the World Flora Online Plant List database.<sup>10</sup> Extracts prepared from the bark, leaves, and roots of this tree are widely used as traditional herbal medicines for the treatment of the common cold, dysentery, malaria, tuberculosis, and cancers.<sup>7,8,11–14</sup> However, the data supporting these medical uses are limited, and the bioactive chemical constituents and mechanisms of action are not well understood.

Several *in vitro* studies suggest that extracts of *T.*

*leiocarpa* exhibit cytotoxicity against various cancer cell lines.<sup>7,15–18</sup> For example, *T. leiocarpa* extracts were cytotoxic against Ehrlich ascites carcinoma cells<sup>15</sup>, HepG2 hepatocarcinoma cells<sup>16</sup>, and breast, gastric, and colon cancer cells.<sup>7,17,18</sup> Previously, we reported that an aqueous partition of a methanol root extract of *T. leiocarpa* (ALRAQ), and isolated ellagic acid (EA) inhibited the proliferation of cultured human ovarian and BC cells, including MCF-7 adenocarcinoma cells.<sup>7</sup> EA (Figure 1) is a naturally occurring polyphenolic compound and is present in many fruits and vegetables, as well as nuts and tree bark.<sup>19,20</sup> It is a dimeric gallic acid derivative produced by the hydrolysis of ellagitannins and originally discovered in oak galls. This compound has significant antioxidant, anti-inflammatory, antimutagenic, and antiproliferative properties in cancer cell lines.<sup>19,20</sup> In our previous work, both ALRAQ and EA treatment of MCF-7 BC cells induced apoptosis, activated caspase 7, and reduced adenosine triphosphate production.<sup>7</sup> Quantitative polymerase chain reaction (qPCR) analysis showed that EA treatment of MCF-7 cells significantly upregulated *BAX* mRNA expression and downregulated *BCL2* mRNA, thereby altering the *BAX/BCL2* ratio in favor of apoptosis.<sup>7</sup>

In this work, we further investigated the molecular mechanisms of action of EA by analyzing its effects on the transcriptome of MCF-7 cells using next-generation RNA sequencing (RNA-seq). Transcriptomic profiling showed that EA significantly altered differential gene expression in MCF-7 cells as compared with controls. Correlation of the RNA-seq data with the Ingenuity Pathway Analysis (IPA) database showed that differential gene expression overlapped with multiple canonical pathways and biological networks associated with cancer, indicating that EA has numerous mechanisms of action.

## 2. Materials and methods

### 2.1. Cell culture and treatment

MCF-7 human mammary adenocarcinoma cells were obtained from the American Type Culture Collection (United States of America [USA]). The cells were subcultured and maintained in minimal essential medium with 10% fetal bovine serum and 1% penicillin/streptomycin and incubated at 37 °C with 5% carbon dioxide as previously described.<sup>7</sup> For the cell viability or RNA extraction assays, MCF-7 cells were treated with an aqueous partition of a methanolic *T. leiocarpa* root extract or its bioactive compound, EA, at the half-maximal inhibitory concentration ( $IC_{50}$ ), and control cells were treated with 0.01% dimethyl sulfoxide (DMSO) in sterile water.<sup>7</sup> The normal cell lines, the human fetal osteoblast cell line and the L6 rat skeletal myoblasts (CRL-1458),

were obtained from the American Type Culture Collection (USA) and cultured and maintained as previously described.<sup>7</sup>

The viability of the BC cells in 96-well plates ( $2.5 \times 10^4$  cells per 100  $\mu$ L/well) was determined using the CellTiter-Glo<sup>®</sup> Luminescent Cell Viability Assay (Promega Corporation, USA) as previously described.<sup>7</sup> Briefly, prior to the addition of the EA (or vehicle solvent, 0.01% DMSO), new medium was added, and the 96-well plates were incubated at 37 °C with 5% carbon dioxide. After incubation for 72 h, the CellTiter-Glo<sup>®</sup> 2.0 Reagent (Promega Corporation, USA) was added to each well, and the plate was processed as described by Lawal *et al.*<sup>7</sup> A Synergy HT Plate reader (Biotek, USA) and Gen5 1.11 software were used to determine the resultant luminescence. The IC<sub>50</sub>s were determined using a log (inhibitor) versus normalized response analysis in GraphPad 10.6.

## 2.2. Preparation, validation, and quantification of mRNA sequencing library

MCF-7 cells were plated at a density of  $1.2 \times 10^6$  cells/mL in 6-well plates and incubated for six hours. The cells were then treated with EA at the IC<sub>50</sub> concentration. After six hours of treatment, the cells were harvested, and total RNA was extracted using TRIzol (Thermo Fisher Scientific, USA) for qPCR analysis and library construction. The RNA samples were checked for purity using NanoDrop<sup>™</sup> One Spectrophotometer (Thermo Fisher Scientific, USA) and analyzed for integrity using 4200 TapeStation (Agilent Technologies, USA). Residual DNA was <10%, as determined by RNA/DNA measurements on a Qubit fluorometer (Thermo Fisher Scientific, USA).

The sequencing libraries were prepared from 250 ng of purified total RNA per sample, using previously described methods.<sup>21,22</sup> Library preparation was performed using the Universal Plus mRNA-seq library preparation kit (Tecan/NuGen, USA). Briefly, RNA underwent poly(A) selection, enzymatic fragmentation, and generation of double-stranded complementary DNA (cDNA) using a mixture of oligo(dT) and random primers. The cDNA underwent end repair, dual-index adaptor ligation, strand selection, and 12 cycles of PCR amplification. All intermediate purification steps, as well as the final amplified library purification, were performed using Agencourt AMPure XPBeads (Beckman Coulter, USA).

Final amplified libraries were measured using the Qubit 1× dsDNA HS assay kit (Invitrogen, USA), and fragment size distribution was confirmed at approximately 430 bp using the D5000 ScreenTape assay (Agilent Technologies, USA). The concentration of the final library pool was confirmed by qPCR and subjected to test sequencing to

assess sequencing efficiency and adjust the proportions of individual libraries accordingly. The pool was quantified by qPCR using the KAPA Library Quantification Kit (Roche Sequencing Solutions, USA) and sequenced on a NovaSeq 6000 S4 flow cell ( $2 \times 150$  bp, approximately 30 M clusters per sample) at the University of Illinois Roy J. Carver Biotechnology Center High-Throughput Sequencing and Genotyping Unit.

## 2.3. Quantitative polymerase chain reaction analysis

RNA was reverse-transcribed and amplified using a Power SYBR Green RNA-to-CT kit (Applied Biosystems, USA) on a StepOne Plus Real Time PCR System (Applied Biosystems, USA), as previously described.<sup>7,21,22</sup> Gene expression was quantified using the  $\Delta\Delta$ CT calculation with  $\beta$ -actin as the endogenous control. Primer sequences (Table 1) were obtained from published works and the National Institutes of Health Primer BLAST.<sup>7,21,22</sup> Data were analyzed using a Student's *t*-test (GraphPad Software 10.6). PCR products were analyzed by electrophoresis on a 1% agarose gel containing ethidium bromide.  $\beta$ -actin was used as a control and to calibrate cDNA synthesis.  $p \leq 0.05$  and false discovery rate ( $q$ ) values of  $\leq 0.05$  were considered statistically significant.

## 2.4. Statistical and bioinformatics analyses

Statistical analyses were performed in GraphPad Prism v10.6. The data are shown as the mean  $\pm$  standard deviation. qPCR analysis was performed using one-way analysis of variance followed by Tukey's or Dunnett's multiple comparison test, with  $p \leq 0.05$  considered statistically significant. IC<sub>50</sub>s were determined using a log (inhibitor) versus normalized response analysis. Next-generation sequencing (mRNA-seq) analyses were performed at the University of Illinois' Core for Research Informatics. FastQC (version 0.12.1), a bioinformatics tool, was used to perform quality control checks on the raw sequencing data using general quality control metrics as previously described.<sup>21,22</sup> FeatureCounts (version 2.0.6), a read summarization program suitable for counting reads generated from RNA, was used to quantify the Ensembl genes, and STAR (version 2.7.11b) was used to align the raw reads to the human reference genome hg38.<sup>23,24</sup> The Ensembl database (www.ensembl.org) was used to analyze the molecular function and biological processes of differentially expressed genes (DEGs) detected from the sequencing data. EdgeR (version 4) was used to calculate the differential expression statistics of raw expression counts using the exactTest function.<sup>25</sup> The obtained  $p$ -values were adjusted for multiple comparisons using the  $q$ -value as described by Benjamini and Hochberg.<sup>26</sup> DEGs were classified into functional clusters using the Gene

Table 1. Primers used for quantitative polymerase chain reaction analyses

Genes	Forward primer sequence (5' to 3')	Reverse primer sequence (5' to 3')
<i>ACTB</i>	TGACGTGGACATCCGCAAAG	CTGGAAGGTGGACAGCGAGG
<i>BID</i>	TGGGACACTGTGAACCAGGAGT	GAGGAAGCCAAACACCAGTAGG
<i>BAX</i>	TGCCAGCAAACCTGGTGCTCA	GCACTCCCGCCACAAAGATG
<i>TP53</i>	AAGTCTGTGACTTGCACGTACTCC	GTCATGTGCTGTGACTGCTTGTAG
<i>ERS1</i>	CTACCTGGAGAACGAGCCCA	AAGGCACTGACCATCTGGTC
<i>JUN</i>	CCGGCTGGAGGAAAAAGT	CCGACGGTCTCTCTTCAA
<i>FOS</i>	CAGAGCATTTGGCAGGAGG	TCTCGGTCTGCAAAGCAG
<i>VIM</i>	AGGCAAAGCAGGAGTCCACTGA	ATCTGGCGTTCCAGGGACTCAT
<i>PTEN</i>	CCGAAAGGTTTGTCTACCATTCT	AAAATTATTTCTTTCTGAGCATTC
<i>BCL2</i>	AGGAGGGACGAACACGTCT	CAAAGAAGGTTGCCCAATCT
<i>BIM</i>	ATGTCTGACTCTGACTCTCG	CCTTGTGGCTCTGTCTGTAG

Ontology (GO) function enrichment analysis in EdgeR.

## 2.5. Ingenuity® Pathway Analysis

Statistically analyzed transcription data were uploaded to the Ingenuity® Pathway Analysis software version 24.0 (Qiagen, USA) as an Excel spreadsheet for analysis. DEGs were analyzed using the predicted protein function in the Ensembl database, and the canonical pathways associated with these changes were identified using previously described methods.<sup>21,22</sup> Upregulation or downregulation of genes and a “core analysis” were performed using a filter based on a log fold change (logFC) of  $\leq -1$  and  $\geq 1$  or a z-score of 3 and a *q*-value  $\leq 0.01$ . The results were then used to identify canonical pathways in the IPA's databases.

## 2.6. Data sharing and availability

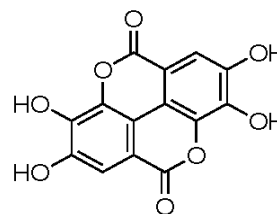
The raw and processed datasets supporting the mRNA-seq conclusions have been deposited in the National Center for Biotechnology Information Gene Expression Omnibus (GEO) repository under the GEO accession GSE221019 (<https://www.ncbi.nlm.nih.gov/geo>).

## 3. Results

### 3.1. Methanol extract of *T. leiocarpa* and ellagic acid-induced cytotoxicity in MCF-7 breast cancer cells

An aqueous partition of a methanol root extract of *T. leiocarpa* and its bioactive compound EA (Figure 1) reduced the viability and proliferation of MCF-7 BC cell growth *in vitro*, with an  $IC_{50}$  of 15.23  $\mu$ g/mL and 28.47  $\mu$ M, respectively. The growth of human osteoblasts or rat L6 myoblasts was not inhibited by either ALRAQ or EA at concentrations up to 100  $\mu$ g/mL. EA was isolated from *T. leiocarpa* using a series of extraction methods, including liquid and column chromatography, and was

identified unambiguously by ultraviolet spectroscopy, mass spectrometry, and  $^1H$  and  $^{13}C$  nuclear magnetic resonance spectra (Figure A1), as previously described.<sup>7</sup> All experimental data agreed with the literature data.



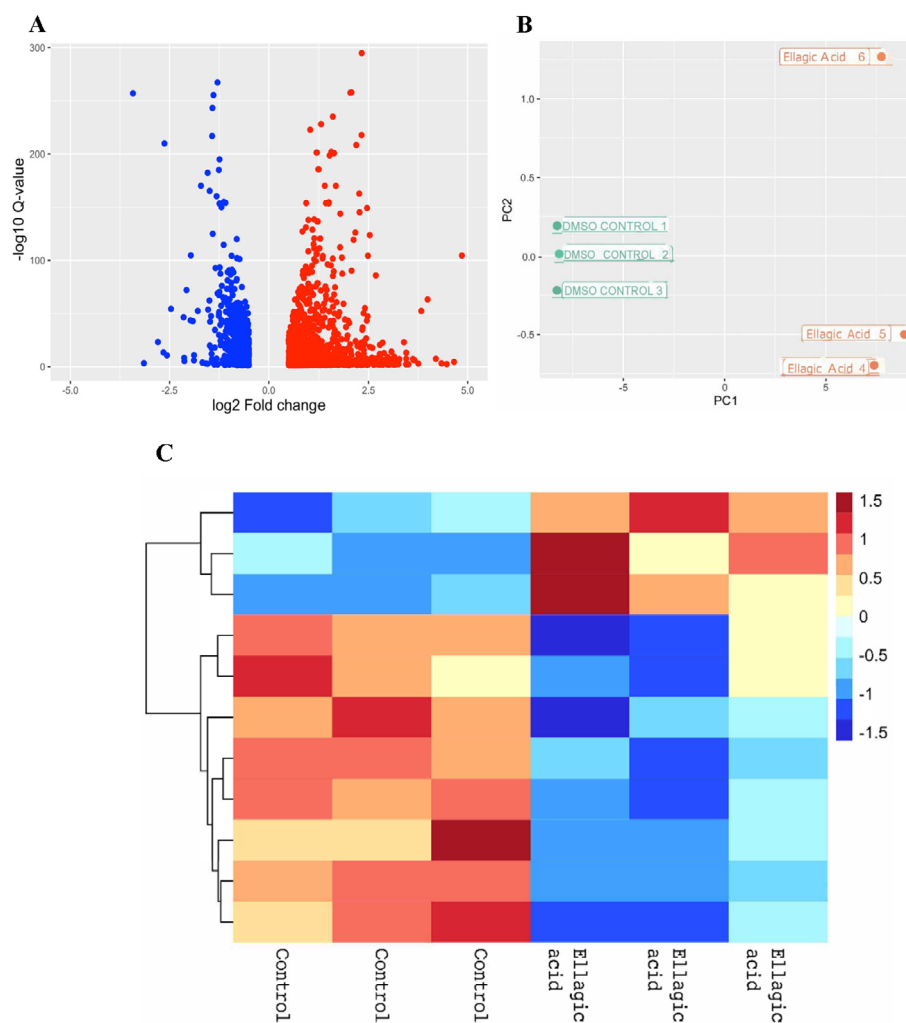
Ellagic acid

Figure 1. Chemical structure of ellagic acid isolated and identified from a *Terminalia leiocarpa* rootbark extract.

### 3.2. Next-generation sequencing of ellagic acid-treated MCF-7 breast cancer cells

To determine the potential molecular mechanisms of action of EA, we performed next-generation sequencing (mRNA-seq) on EA-treated MCF-7 cells using total RNA harvested from control and treated cells. RNA quality was measured on the 4200 TapeStation, and each RNA sample had an RNA integrity number of 9.5–10. The RNA samples were used to prepare RNA-seq libraries with a Universal Plus mRNA-seq kit. After amplification, the libraries were purified, and the fragment distribution ranged from 430 bp, as determined by electrophoresis. The purified libraries were normalized and pooled to a final concentration of 10 nM. Bioinformatic analysis of the RNA-seq data showed that of 26,048 genes screened, 4,848 were differentially expressed, with 2,180 transcripts upregulated and 2,668 downregulated ( $q \leq 0.01$ ).

A volcano plot of the 4,848 DEGs impacted by EA treatment of MCF-7 cells is depicted in Figure 2A. The



**Figure 2.** Gene expression analyses. (A) A volcano plot depicting the relationship between the magnitude of gene expression changes (x-axis:  $\log_2$  fold change) and their statistical significance (y-axis:  $-\log_{10}$  of the false discovery rate,  $q$ -value) for the 4,848 differentially expressed genes ( $q \leq 0.05$ ) in treated versus control MCF-7 breast cancer cells. Each point represents one transcript based on the average of three replicates. Points were colored according to their expression in the dataset, with blue indicating downregulated genes and red indicating upregulated genes. (B) Principal component analysis (PCA) of control MCF-7 cells (treated with 0.01% dimethyl sulfoxide [DMSO],  $n = 3$ ) or ellagic acid (EA)-treated MCF-7 cells ( $n = 3$ ). The green dots represent 0.01% DMSO control cells, and the red dots represent EA-treated MCF-7 cells. (C) Heatmap analysis of the top 11 differentially expressed genes with gene ontology across datasets. MCF-7 cells treated with EA ( $IC_{50}$ ) and compared with controls (0.01% DMSO), using  $q \leq 0.01$  and  $\log_2$  fold change of  $\leq -3$  or  $\geq 3$ . Each column in the graph depicts the value for one replicate, three for controls, and three for EA-treated cells. Light to dark blue indicates downregulated transcripts, and red, orange, and yellow indicate upregulated transcripts.

gene expression pattern is scattered outward away from the center of origin. Downregulated DEGs (2,668) are depicted in blue, while upregulated DEGs (2,180) are depicted in red. Figure 2B depicts the principal component analysis of control MCF-7 cells treated with 0.01% DMSO ( $n = 3$ ) versus EA-treated MCF-7 cells ( $n = 3$ ). The green dots represent the 0.01% DMSO control, and the red dots depict EA-treated MCF-7 cells. Figure 2C depicts a heatmap of the top 11 DEGs with GO across datasets, using  $q \leq 0.01$  and  $\log_2$  FC of  $\leq -3$  or  $\geq 3$ . In MCF-7 cells, treatment with EA or 0.01% DMSO (control) showed distinct gene expression

patterns, demonstrating the data's reliability, with yellow, orange, and red indicating upregulated transcripts and light to dark blue indicating downregulated transcripts. The statistical analyses of the RNA-seq data were performed using the EdgeR exact test, and the  $p$ -values were adjusted for multiple comparisons using the  $q$ -value via the Benjamini–Hochberg algorithm.<sup>26</sup>

The abbreviations, names, and data of the top 10 upregulated and downregulated genes are presented in Tables 2 and 3.



**Table 2. Top ten upregulated genes in ellagic acid-treated MCF-7 breast cancer cells**

Genes	Name	Ensembl ID	Log fold change
<i>LSP1</i>	Lymphocyte-specific protein 1 gene	ENSG00000130592	6.080
<i>ISM1</i>	Isthmin-1	ENSG00000101230	5.780
<i>PLAAT4</i>	Phospholipase A and acyltransferase 4	ENSG00000133321	5.780
<i>KLF14</i>	KLF transcription factor 14	ENSG00000266265	5.510
<i>RP11_274B2110</i>	Long noncoding RNA	ENSG00000230715	5.170
<i>VSX2</i>	Visual system homeobox 2	ENSG00000119614	5.170
<i>PAH</i>	Phenylalanine hydroxylase	ENSG00000171759	4.640
<i>SULT4A1</i>	Sulfotransferase family 4A member 1	ENSG00000130540	4.160
<i>MT4</i>	Metallothionein 4	ENSG00000102891	4.070
<i>IGHA1</i>	Immunoglobulin heavy constant alpha 1	ENSG00000211895	4.060

**Table 3. Top ten downregulated genes in ellagic acid-treated MCF-7 breast cancer cells**

Genes	Name	Ensembl ID	Log fold change
<i>INHBE</i>	Inhibin subunit beta E	ENSG00000139269	-8.230
<i>NLRP1</i>	NLR family pyrin domain-containing 1	ENSG00000091592	-8.020
<i>LOC101927914</i>	Pseudo gene	ENSG00000234210	-7.930
<i>KLHDC7B</i>	Kelch domain-containing 7B	ENSG00000130487	-7.810
<i>AC006372.5</i>	Linc RNA	ENSG00000223872.1	-7.750
<i>IFNLR1</i>	Interferon lambda receptor 1	ENSG00000185436	-7.450
<i>CYBRD1</i>	Cytochrome b reductase 1	ENSG00000071967	-7.420
<i>SERPINA3</i>	Serpin family A member 3	ENSG00000196136	-7.000
<i>FGF21</i>	Fibroblast growth factor 21	ENSG00000105550	-6.970
<i>SETBP1</i>	SET binding protein 1	ENSG00000152217	-6.940

### 3.3. Ingenuity Pathway Analysis of next-generation sequencing data of ellagic acid-treated MCF-7 cells

To investigate novel mechanisms of action, IPA was used to determine the overlap between DEGs from RNA-seq data for EA-treated and control MCF-7 cells with canonical pathways and biological networks in the IPA database. For this analysis, 2,518 DEGs with a  $\log_2FC$  of  $\leq -1$  or  $\geq 1$  and  $q \leq 0.01$  were used. To determine if there was a significant correlation between specific canonical pathways and DEGs, IPA and the Ensembl database were used. IPA core analysis showed that significant changes in DEG expression overlapped with 98 canonical pathways in EA-treated MCF-7 BC cells compared with control cells, of which 56 are shown in the volcano bubble plot in [Figure 3](#). A graph of the top 13 canonical pathways affected by EA treatment in MCF-7 cells compared with controls is shown in [Figure 4](#). The most significant canonical pathways associated with EA-treated BC cells included apoptosis signaling, estrogen receptor signaling, estrogen-dependent BC signaling, and regulation of the epithelial-to-mesenchymal transition

(EMT), suggesting that EA has multiple mechanisms of action in MCF-7 cells. [Table 4](#) presents the most significant diseases and biological functions predicted to be affected by EA, including  $p$ -values and the number of affected molecules. Not surprisingly, cancer was the most affected disease state, along with endocrine and reproductive disorders and diseases.

### 3.4. Upregulation of canonical pathways for apoptosis and molecular mechanisms in cancer in ellagic acid-treated MCF-7 cells

To determine novel mechanisms of action associated with the effects of EA on MCF-7 cells, the overlap of statistically significant DEGs ( $q \leq 0.01$ ) with interconnecting and specific canonical pathways related to BC was analyzed using bioinformatics coupled with IPA. Network analysis in treated MCF-7 cells showed that EA treatment downregulated multiple interconnected genes and signaling pathways associated with cancer ([Figure 5](#)). Transcriptomic analysis of EA-treated MCF-7 cells showed that, as compared with control cells, EA-treated MCF-7



**Figure 3.** A volcano bubble plot depicting the upregulation or downregulation of 62/98 canonical pathways and z-score impacted in ellagic acid (EA)-treated MCF-7 breast cancer cells. The plot shows significant downregulation in numerous canonical pathways associated with cancer, including estrogen-dependent breast cancer signaling, estrogen-mediated S phase entry, human epidermal growth factor receptor 2 signaling in breast cancer, estrogen receptor signaling, and others. The canonical pathways are depicted as bubbles, with bubble size indicating the number of genes overlapping the pathway. The color of the bubbles represents the z-scores, with blue indicating downregulated pathways and red/orange indicating upregulated pathways. Multiple canonical pathways were altered in EA-treated MCF-7 breast cancer cells, with apoptosis signaling pathways significantly upregulated and estrogen signaling pathways significantly downregulated. Only differentially expressed genes with a  $|\log_2 \text{fold change}| \geq 1$  ( $q \leq 0.01$ ) were included in the plot.

**Table 4. Top diseases and biological functions impacted by ellagic acid in cultured MCF-7 breast cancer cells**

Name	p-value range	Number of molecules
Cancer	$1.16 \times 10^{-6}$ – $6.20 \times 10^{-140}$	2,162
Organismal injury and abnormalities	$1.16 \times 10^{-6}$ – $6.20 \times 10^{-140}$	2,187
Gastrointestinal disease	$1.13 \times 10^{-6}$ – $3.18 \times 10^{-84}$	1,932
Endocrine system disorders	$1.08 \times 10^{-6}$ – $1.29 \times 10^{-83}$	1,857
Reproductive system disorders	$1.08 \times 10^{-6}$ – $2.43 \times 10^{-50}$	1,557

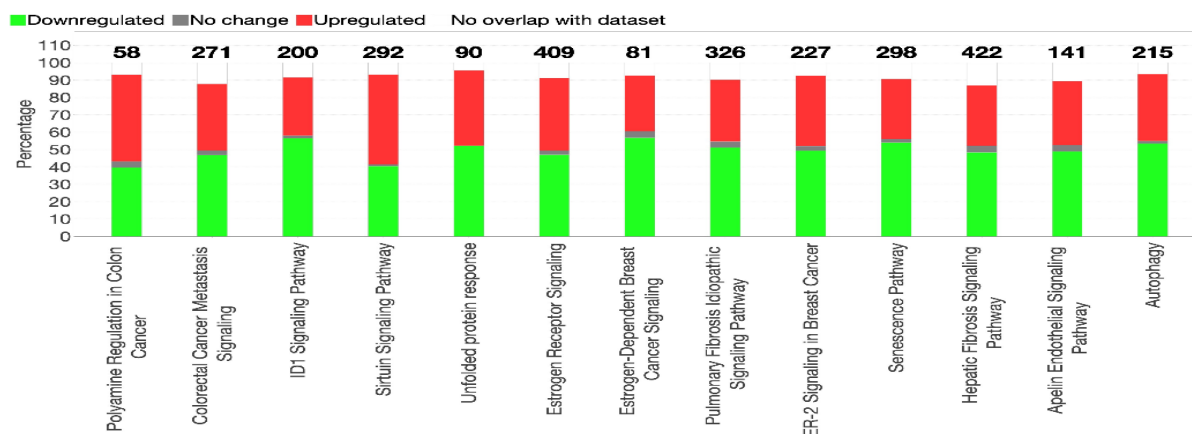


**Figure 4.** The top 13 canonical pathways altered by ellagic acid treatment of MCF-7 breast cancer cells. The chart was generated using Ingenuity Pathway Analysis, with a  $|\log_2 \text{ fold change}| \geq 1$  ( $q \leq 0.01$ ). The graph shows the names of the pathways, the number of genes in each, and the percentage of up- or downregulated genes. Significant overlap in gene expression was observed in the estrogen receptor signaling, estrogen-dependent breast cancer signaling, human epidermal growth factor receptor 2 (HER2) signaling in breast cancer and metastasis canonical pathways, indicating significant ( $q \leq 0.01$ ) downregulation.

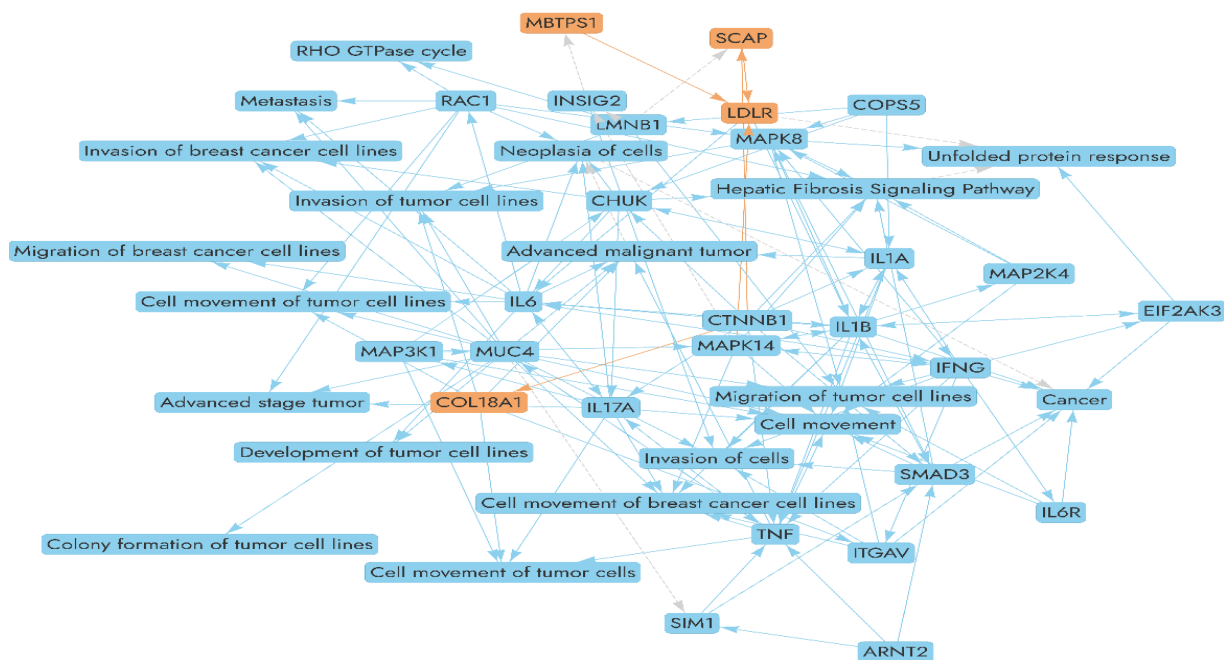


**Figure 5.** Graphical summary and network analysis of the predicted interconnecting canonical pathways and genes impacted by ellagic acid (EA)-treated MCF-7 breast cancer cells. The chart indicates coordinated suppression of tumor progression and inflammation through multi-pathway gene regulation. The network reveals that EA decreases the expression of specific genes (e.g., *MUC4*, *IL1A*, *IL6*, *ITGAV*, *RAC1*) and increases *COL18A1* expression, thereby reducing processes central to cancer progression, including cell movement, invasion, metastasis, and migration in MCF-7 cells. Pathways and genes highlighted in orange show significant upregulation, while those highlighted in blue indicate significant downregulation. The analysis was performed in Ingenuity Pathway Analysis using  $|\log_2 \text{ fold change}| \geq 1$  ( $q \leq 0.01$ ).



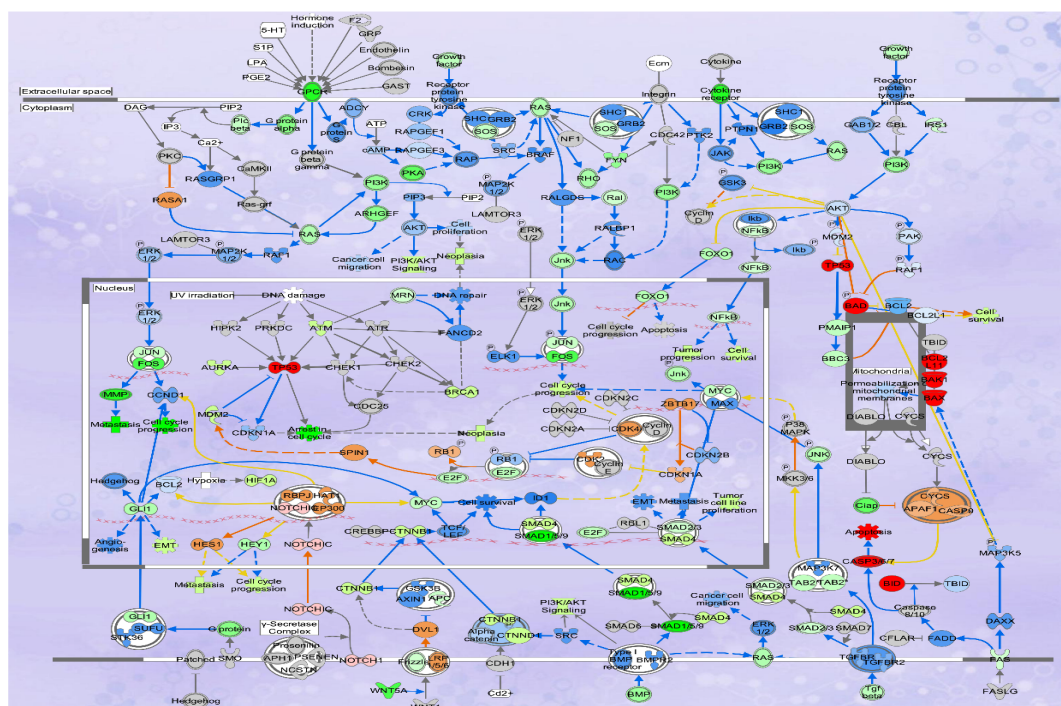


**Figure 6.** Pathway analysis of the canonical pathway “molecular mechanisms in cancer.” Ellagic acid-treated MCF-7 cells altered differential gene expression across many signaling pathways, which overlapped with the molecular mechanisms of the cancer canonical pathway. Treatment altered the expression of 132 of 447 genes in this pathway ( $|\log_2 \text{ fold change}| \geq 1$  [ $q \leq 0.01$ ]). The genes/functions highlighted in red/pink show significant experimental upregulation, while genes/pathways highlighted in green/light green show significant downregulation. Genes and functions shown in blue/orange are predicted and generated using the Ingenuity Pathway Analysis prediction function.

cells significantly ( $\log_2 \text{FC}$  of  $\leq -3$  or  $\geq 3$ ,  $q \leq 0.01$ ) altered expression of transcripts associated with “molecular mechanisms in cancer” canonical pathway (Figure 6). Significant upregulation of DEGs related to apoptosis, including *BAX*, *BAD*, *BID*, and *BAK*, as well as the tumor suppressors *TP53* and *PTEN*, was observed (Figure 6). Validation of gene expression was performed using qPCR (Figure A2).

### 3.5. Downregulation of estrogen receptor signaling, estrogen-dependent breast cancer signaling, and the epithelial-to-mesenchymal transition canonical pathways in ellagic acid-treated MCF-7 cells

Two of the most significantly downregulated canonical pathways associated with BC included estrogen receptor signaling, estrogen-dependent BC signaling, and the EMT pathways (Figures 7 and 8). Thirty-three genes were differentially expressed in the estrogen-dependent BC signaling pathway in EA-treated MCF-7 cells. Significant ( $q \leq 0.01$ ) downregulation of *ESR1*, *EGFR*, *FOS*, and *JUN* was observed in this signaling pathway (Figure 7). In the EMT canonical pathway, 55 of 192 genes were

differentially expressed ( $q \leq 0.01$ ) (Figure 8), including the downregulation of *VIM*, *TWIST1*, *PRRX1/2*, *FOS*, and *EGR1*, which are involved in the EMT. *PRRX1* is a key EMT gene, and elevated expression is associated with BC development and progression, as well as a poor prognosis, tumor invasion, and metastasis. Finally, gene expression in the *PDGFR* signaling network was significantly ( $q \leq 0.01$ ) downregulated (Figure 9).

Gene expression of *IL1A*, *IFN*, *IL6*, *IL17A*, and *TNF* was also downregulated in EA-treated MCF-7 cells. Increased expression of these genes has been linked to advanced malignant tumors. The transcripts for *MAP3K1*, *RAC1*, and *ITGAV* were also significantly downregulated. Overexpression of the *MAP3K1* and *ITGAV* genes has been linked with an increased risk of BCs, as well as the progression of cancer, making them a target for research and potential therapeutic development. Thus, transcriptomic analysis indicates that EA significantly downregulated the expression of many genes involved in cell movement, invasion, and metastasis in MCF-7 cells, supporting previous reports that EA may reduce BC invasiveness and metastasis.

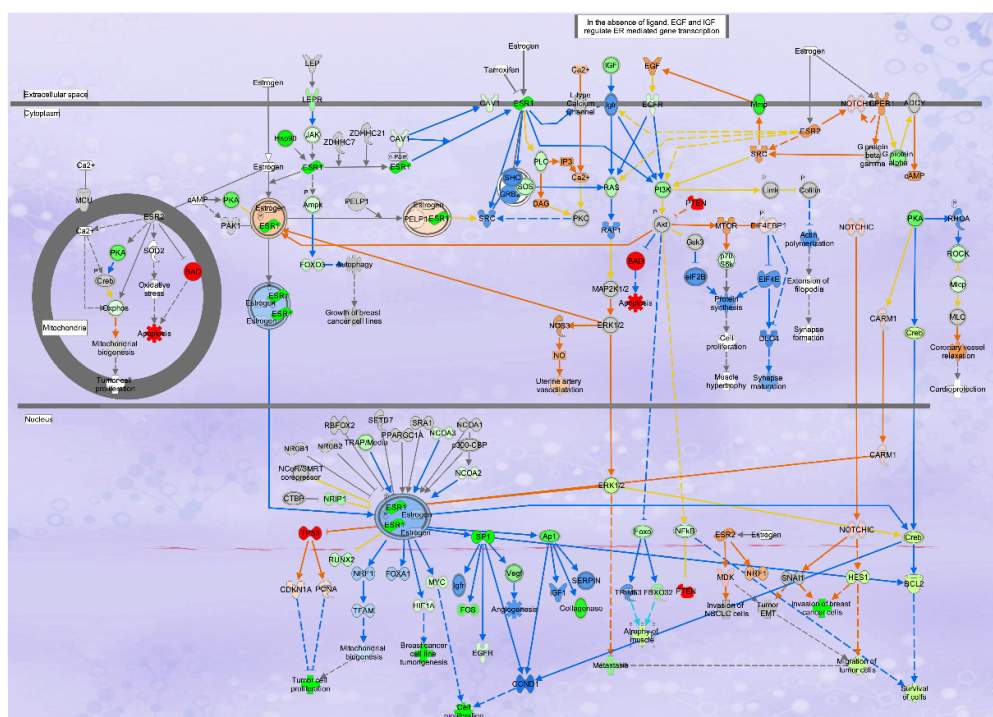


**Figure 7.** Ellagic acid (EA) treatment of MCF-7 breast cancer cells downregulated estrogen-dependent signaling and upregulated apoptosis. In this canonical pathway, EA treatments significantly altered the expression of 33 of the 83 genes ( $q \leq 0.01$ ). Significant downregulation of the estrogen receptor 1 (*ESR1*), epidermal growth factor receptor (*EGFR*), c-FOS (*FOS*), and c-JUN (*JUN*) was observed in this signaling pathway. The genes/functions highlighted in red/pink show significant experimental upregulation, while genes/pathways highlighted in green/light green show significant downregulation. Genes and functions shown in blue are predicted and generated using the Ingenuity Pathway Analysis software prediction function. Only genes with  $|\log_2$  fold change  $\geq 1$  ( $q \leq 0.01$ ) were included.

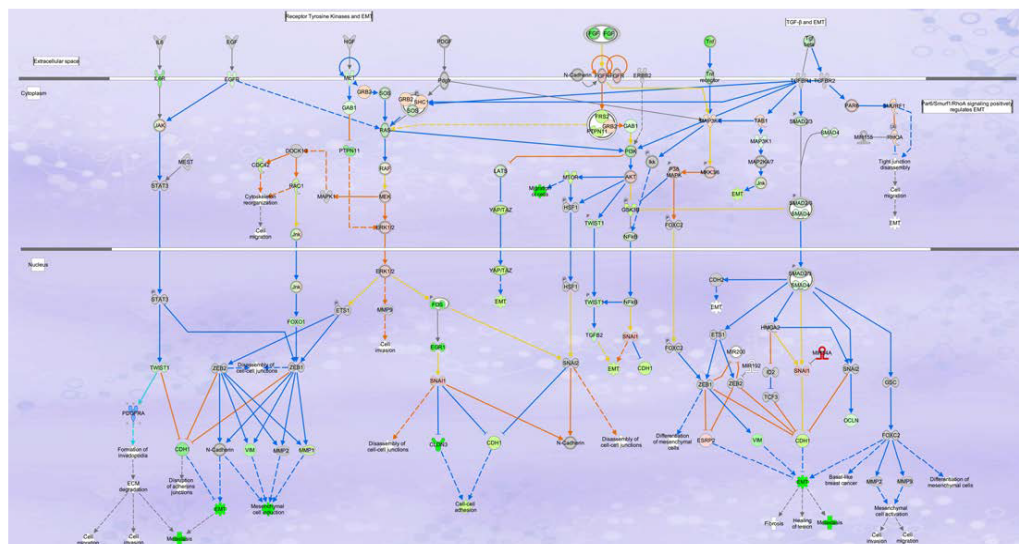


**Figure 8.** Downregulation of the epithelial-to-mesenchymal transition (EMT) canonical pathway. Ellagic acid-treated MCF-7 breast cancer cells significantly ( $z$ -score:  $-2.59$ ;  $p = 4.24 \times 10^{-4}$ ) downregulated genes involved in EMT. Significant downregulation of the transcripts for *VIM*, *TWIST1*, *PRRX1/2*, *FOS*, and *EGR1* was observed ( $q \leq 0.01$ ). Genes highlighted in red/pink show significant experimental downregulation, while genes highlighted in green/light green show significant experimental upregulation ( $q \leq 0.01$ ). Genes and functions shown in blue (downregulated) or orange (upregulated) were estimated using the prediction function in Ingenuity Pathway Analysis. Fifty-five of the 192 genes in this pathway were differentially expressed after treatment; however, only those with  $|\log_2$  fold change  $\geq 1$  ( $q \leq 0.01$ ) were included.

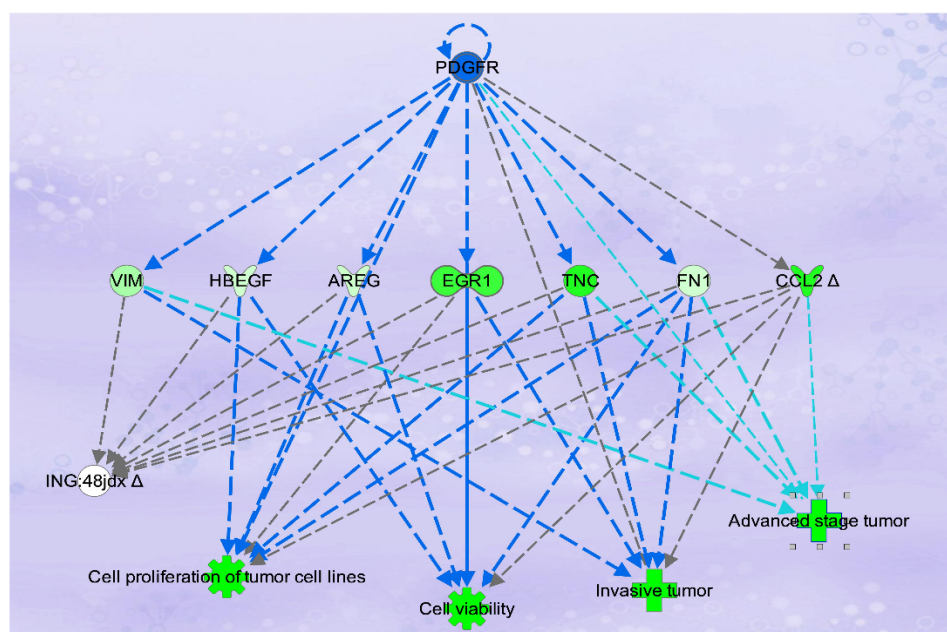


**Figure 9.** Experimental downregulation of gene expression in the platelet-derived growth factor receptor (*PDGFR*) signaling pathway induced by ellagic acid treatment of MCF-7 breast adenocarcinoma cells. Multiple cancers, including breast, gliomas, Kaposi's sarcoma, prostate, ovarian, renal cell, and pancreatic cancers, have been associated with persistently elevated levels of PDGFs and PDGFRs in cancer cells. *VIM* was downregulated by 4-fold ( $q \leq 0.01$ ); *AREG* was downregulated by 2-fold ( $q \leq 0.01$ ); *EGR1* was downregulated by 8.5-fold ( $q \leq 0.01$ ); *TNC* was downregulated by 10.7-fold ( $q \leq 0.01$ ); and *CCL2* was downregulated by 10.98-fold ( $q \leq 0.01$ ). Genes depicted in green represent experimentally derived data, while genes in blue are predicted using the prediction function in Ingenuity Pathway Analysis.

#### 4. Discussion

Breast cancer remains a leading cause of morbidity and mortality in women worldwide.<sup>27–29</sup> While Western medicines are commonly available, many patients in Africa still choose to incorporate traditional plant-based medicines into their therapeutic regimen. Extracts of one such plant, *Terminalia leiocarpa*, have been used as a traditional medicine for the treatment of many diseases, including cancers. Many naturally occurring phenolic compounds, including EA, have been isolated from extracts of this tree and reported to have anticancer activities.<sup>7,30–40</sup> *In vitro* and *in vivo* studies of EA have demonstrated that it reduced the proliferation of breast, bladder, leukemia, melanoma, pancreatic, and prostate cancer cells.<sup>7,32–40</sup> For example, in pancreatic cancer, EA reduced PANC-1 cell proliferation and migration *in vitro* and reduced tumor load in xenograft mouse models.<sup>32</sup> In PANC-1 cells, EA also increased cell cycle arrest, downregulated *VIM* gene expression, and suppressed the EMT.<sup>32</sup> In androgen-dependent prostate cancer cells, EA isolated from pomegranate juice induced intrinsic apoptosis, downregulated anti-apoptotic *BCL2* mRNA expression, upregulated pro-apoptotic *BAX* mRNA expression, and increased caspase activities.<sup>34</sup> In bladder cancer cells, EA increased apoptosis, induced cell cycle

arrest, and increased the expression of tumor suppressors *p53/p21* and *VEGF*.<sup>35</sup> In the human BC cell lines MCF-7, MDA-MB-231, and BT-474, EA reduced cell proliferation and induced apoptosis.<sup>7,36–38</sup> In these previous studies, the  $IC_{50}$  of EA in MCF-7 cells ranged from 20  $\mu M$  to 30  $\mu M$ .<sup>7,35–37</sup> In this study, the  $IC_{50}$  of EA isolated from *T. leiocarpa* was 28.47  $\mu M$  in MCF-7 cells, within the range of previously reported concentrations.

In terms of anticancer mechanisms of action, EA activated tumor suppressors and upregulated the expression of B-cell lymphoma 2 pro-apoptotic proteins in various BC cell lines.<sup>35,37–40</sup> In addition, EA-treated MCF-7 cells induced apoptosis and cell cycle arrest by altering transforming growth factor-beta/SMAD family member 3 signaling<sup>39</sup> and by inhibiting cyclin-dependent kinase 6.<sup>40</sup> In cultured estrogen receptor-positive (ER+) MCF-7 and estrogen receptor-negative (ER-) MDA-MB-231 BC cells, EA exerted anti-angiogenesis effects via the vascular endothelial growth factor receptor 2 signaling pathway, as well as reduced tumor load in MDA-MB-231 xenografts.<sup>42</sup>

In our previous work, we demonstrated that an aqueous partition of a *T. leiocarpa* root extract and isolated EA reduced the proliferation of MCF-7 BC cells by inducing apoptosis and autophagy.<sup>7</sup> To further



investigate novel mechanisms of action, we analyzed the whole transcriptome using next-generation sequencing (RNA-seq) in EA-treated MCF-7 cells. EA treatment induced differential expression of 4,848 transcripts, with 2,180 genes upregulated and 2,668 genes downregulated ( $q \leq 0.01$ ). Bioinformatic and Ingenuity Pathway analyses of the RNA-seq datasets revealed significant alterations in differential gene expression that overlapped with specific canonical pathways associated with BC. EA treatment of MCF-7 cells significantly upregulated gene expression in apoptosis canonical signaling, downregulated estrogen receptor signaling, downregulated estrogen-dependent BC and HER2+ signaling pathways, and downregulated gene expression in the EMT canonical pathway. These data suggest that EA has multiple mechanisms of action in ER+ MCF-7 BC cells.

In a previous work, Papoutsi *et al.*<sup>43</sup> reported that EA exhibited antiestrogenic effects in HeLa cells transfected with an estrogen response element-driven luciferase reporter gene and E $\alpha$  or ER $\beta$  expression vectors. In the study, EA acted as a potent antiestrogen in transfected HeLa and MCF-7 cells, with activity similar to that of the estrogen antagonist ICI182780.<sup>43</sup> Our work supports these results and further shows that EA significantly downregulated the expression of the *ESR1*, *HSD17B11*, and *HSD17B7* genes involved in estrogen biosynthesis and signaling. The enzyme complex 17 $\beta$ -hydroxysteroid dehydrogenase (17 $\beta$ -HSD) plays a key role in estrogen biosynthesis by converting estrone (E1) into the active form estradiol (E2).<sup>44–47</sup> Wang *et al.*<sup>45</sup> demonstrated that silencing both *HSD17B11* and *HSD17B7* in T47D: A18 and MCF-7 cells inhibited the growth of these cells, indicating that these enzymes play a central role in BC cell growth. Thus, downregulation of 17 $\beta$ -HSD and *ESR1* transcripts in EA-treated MCF-7 cells may be one of the mechanisms by which EA reduces BC cell proliferation. Since the expression of *HSD17B11*, *HSD17B5*, and *HSD17B7* is increased in BC, their enzymes could serve as novel targets for BC chemotherapy.<sup>44</sup> Interestingly, our data also showed that EA treatment of MCF-7 cells significantly ( $q \leq 0.01$ ) downregulated gene expression in the HER2+ canonical signaling pathway, suggesting that investigations of the effects of EA in HER2+ cancers could be a focus of future research.

Beyond estrogen signaling, EA also significantly ( $q \leq 0.01$ ) downregulated the expression of key genes in the EMT canonical pathway, including *VIM*, *TGF*, *PRRX1/2*, *TWIST1*, and *FOS* in MCF-7 cells. The EMT is a complex, reversible signaling pathway that enables epithelial cells to adopt a mesenchymal phenotype, allowing them to invade surrounding tissues and thereby increase cancer

metastasis.<sup>48–50</sup> The EMT is regulated by numerous genes, including *TWIST1* and *VIM*.<sup>48–52</sup> Previous investigations have shown that upregulation of *TWIST1* expression decreased apoptosis, and increased EMT and cancer metastasis.<sup>48–52</sup> In the EMT signaling cascade, *TWIST1* activation upregulates vimentin through a mechanism that is not well understood.<sup>48,49</sup> Vimentin (encoded by the *VIM* gene) is an intermediate filament structural protein expressed in mesenchymal cells and plays a key role in cellular attachment, signaling, and cancer cell migration.<sup>50–52</sup> EA treatment of MCF-7 cells also downregulated the expression of *PRRX1* and 2 mRNA, which are also involved in the EMT. The paired-related homeobox 1 (*PRRX1*) is a key transcription factor that plays a significant role in cancer progression by acting as a “master regulator” of cancer-associated fibroblasts, promoting tumor growth and metastasis.<sup>53</sup> Overexpression of these genes has been associated with the development and progression of BC and with poor prognosis, tumor invasion, and metastasis.<sup>53</sup> EA treatment of MCF-7 cells also downregulated the platelet-derived growth factor receptor (*PDGFR*) signaling pathway. The *PDGFRA* gene encodes a cell surface receptor tyrosine kinase whose activity is required for EMT progression. Downregulation of this signaling pathway has been shown to reduce cancer cell proliferation and invasion, making it a promising new target for cancer chemotherapy.<sup>54</sup> Suppression of the EMT by EA has also been observed in cultured gastric and pancreatic cancer cell lines.<sup>32,55</sup> Lim *et al.*<sup>55</sup> reported that EA treatment of gastric carcinoma cells suppressed EMT by downregulating the expression of *TGF*, matrix metalloproteinases, *SNAIL*, *TWIST1*, and *c-myc* genes. In PANC-1 cells, EA also suppressed EMT by upregulating E-cadherin and downregulating *VIM* expression.<sup>32</sup> Thus, our data also supported previous work and further suggest that EA significantly affects genes in the EMT signaling pathway in BC cells, warranting more thorough investigation for the prevention and treatment of metastatic breast disease.

## 5. Conclusion

In Africa, ALRAQ is used in traditional medicine to treat infections and cancers. In a previous work, we identified one of the active chemical constituents of ALRAQ, EA, a known compound with anticancer activities. EA induced apoptosis in MCF-7 BC cells and significantly reduced estrogen signaling. Transcriptomic analysis showed that EA inhibited the growth of human MCF-7 BC cells by altering gene expression in multiple cancer-related canonical pathways, including apoptosis, estrogen signaling, and EMT. Since estrogens are the driving force for the progression of HR+ cancers, therapies that reduce

estrogen synthesis and signaling are important for both prevention and treatment. In addition, downregulation of the EMT suggests that EA (and ALRAQ) may reduce BC progression and metastasis. Thus, EA and ALRAQ have plausible mechanisms of action for the treatment of BC and warrant further investigation as adjunct therapies to prevent metastatic disease.

## Acknowledgments

We would like to thank the staff of the UIC Genomics and Research Informatics Cores for their thoughtful discussions and support of this work. The contents are solely the responsibility of the authors and do not necessarily represent the official views of the funding agencies.

## Funding

This work was funded by a Schlumberger Faculty of the Future Foundation Fellowship award to TOL. PK and MMC were supported partly by the University of Illinois at Chicago (UIC) Center for Clinical and Translational Science (CCTS) under Grant #UL1TR002003 from the National Center for Advancing Translational Sciences, National Institutes of Health. The funding agency had no role in the design of the study, the collection, analysis, or interpretation of data, or the writing of the manuscript.

## Conflict of interest

The authors declare that they have no competing interests.

## Author contributions

**Conceptualization:** Gail B. Mahady, Temitope O. Lawal, Bolanle A. Adeniyi

**Formal analysis:** Gail B. Mahady, Pinal N. Kanabar, Mark Maienschein-Cline

**Funding acquisition:** Gail B. Mahady, Temitope O. Lawal, Mark Maienschein-Cline, Pinal N. Kanabar

**Investigation:** Temitope O. Lawal, Pinal N. Kanabar, Nina S. Los, Shitalben M. Patel, Zarema H. Arbueva, Gail B. Mahady

**Methodology:** Pinal N. Kanabar, Nina S. Los, Shitalben M. Patel, Zarema H. Arbueva, Gail B. Mahady

**Writing-original draft:** Gail B. Mahady, Temitope O. Lawal, Bolanle A. Adeniyi, Mark Maienschein-Cline

**Writing-review & editing:** Gail B. Mahady, Temitope O. Lawal, Bolanle A. Adeniyi, Mark Maienschein-Cline

## Ethics approval and consent to participate

Not applicable.

## Consent for publication

Not applicable.

## Availability of data

The raw and processed datasets supporting the mRNA-seq conclusions have been deposited in the National Center for Biotechnology Information Gene Expression Omnibus (GEO) repository under the GEO accession GSE221019 (<https://www.ncbi.nlm.nih.gov/geo>).

## References

1. World Health Organisation: Breast cancer factsheet. Updated 2025. Available from: <https://www.who.int/news-room/fact-sheets/detail/breast-cancer> [Last accessed on 2025 May 24].
2. Azubuike SO, Muirhead C, Hayes L, McNally R. Rising global burden of breast cancer: the case of sub-Saharan Africa (with emphasis on Nigeria) and implications for regional development: a review. *World J Surg Onc.* 2018;16: 63.  
doi: 10.1186/s12957-018-1345-2
3. Adeboye D, Sowunmi OY, Jacobs W, David RA, Adeosun AA, Amuta AO, Misra S, Gadanya M, Auta A, Harhay MO, Chan KY. Estimating the incidence of breast cancer in Africa: a systematic review and meta-analysis. *J Glob Health.* 2018;8(1):010419.  
doi: 10.7189/jogh.08.010419.
4. Onyia AF, Nana TA, Adewale EA, et al. Breast cancer phenotypes in Africa: A scoping review and meta-analysis. *JCO Glob Oncol.* 2018;9:e2300135.  
doi: 10.1200/GO.23.00135.
5. Ntekim A, Oluwasanu M, Odukoya O. Breast cancer in adolescents and young adults less than 40 years of age in Nigeria: A retrospective analysis. *Int J Breast Cancer.* 2022;2022:9943247.  
doi: 10.1155/2022/9943247.
6. Asuzu CC, Akin-Odanye EO, Asuzu MC, Holland J. A socio-cultural study of traditional healers' role in African health care. *Infect Agent Cancer.* 2019;14:15.  
doi: 10.1186/s13027-019-0232-y.
7. Lawal TO, Patel S, Raut N, Mahady GB. Extracts of *Anogeissus leiocarpus* and *Dillenia indica* inhibit the growth of MCF-7 breast cancer and COV434 granulosa tumour cells by inducing apoptosis and autophagy. *Current Bioactive Compounds.* 2021;17:e190721191390.  
doi: 10.2174/1573407217666210215092955
8. Odumosu BT, Kolude B, Adeniyi BA. Antimicrobial screening and kinetic study of two Nigerian medicinal plants against oral pathogens. *CIBTech J Pharm Sci.* 2014;3(2): 7-14.
9. Ezeome ER. Delays in presentation and treatment of breast cancer in Enugu, Nigeria. *Niger J Clin Pract.* 2010;13(3):



- 311–316.
10. WFO Plant List: Snapshots of the Taxonomy. Available from: <https://www.WFOplantlist.org> [Last accessed on 2025 May 06].
11. Adekunle YA, Samuel BB, Nahar L, Fatokun AA, Sarker SD. *Anogeissus leiocarpus* (DC.) Guill. & Perr. (Combretaceae): A review of the traditional uses, phytochemistry and pharmacology of African birch. *Fitoterapia*. 2024;176: 105979.  
doi: 10.1016/j.fitote.2024.105979.
12. Micheli L, Ferrara V, Akande T, *et al.* Ellagitannins and triterpenoids extracts of *Anogeissus leiocarpus* stem bark extracts: Protective effects against osteoarthritis. *Phytother Res*. 2023;37(6):2381–2394.  
doi: 10.1002/ptr.7760.
13. Singh D, Baghel US, Gautam A, *et al.* The genus *Anogeissus*: A review on ethnopharmacology, phytochemistry and pharmacology. *J Ethnopharmacol*. 2016;194:30–56.  
doi: 10.1016/j.jep.2016.08.025.
14. Arbab AH. Review on *Anogeissus leiocarpus* a potent African traditional drug. *Int J Res Pharm Chem*. 2014;4:496–500.
15. Salau AK, Yakubu MT, Oladiji, AT. Cytotoxic activity of aqueous extracts of *Anogeissus leiocarpus* and *Terminalia avicennioides* root barks against Ehrlich ascites carcinoma cells. *Indian J Pharmacol*. 2013;45(4):381–385.  
doi: 10.4103/0253-7613.115023
16. Olugbami JO, Damoiseaux R, France B, *et al.* A comparative assessment of antiproliferative properties of resveratrol and ethanol leaf extract of *Anogeissus leiocarpus* (DC) Guill and Perr against HepG2 hepatocarcinoma cells. *BMC Complement Altern Med*. 2017;17(1).  
doi: 10.1186/s12906-017-1873-2
17. Hassan LEA, Al-Suede FS, Fadul SM, Abdul Majid AMS. Evaluation of antioxidant, antiangiogenic and antitumor properties of *Anogeissus leiocarpus* against colon cancer. *Angiotherapy*. 2018;1(2):56–66.  
doi: 10.25163/angiotherapy.1200021526100818
18. Lawal TO, Patel S, Mahady, GB. Food and medicinal plants from Nigeria with anti-*Helicobacter pylori* activities induce apoptosis in colon and gastric cancer cell lines. *Functional Foods in Health and Disease*. 2023;13(7):372–387.  
doi: 10.31989/ffhd.v13i7.1105
19. Seigler, DS. *Plant Secondary Metabolism*. Kluwer Academic Publishers, Springer Science & Business Media. 1998:208.
20. Golmei P, Kasna S, Roy KP, Kumar S. A review on pharmacological advancement of ellagic acid. *J Pharmacol Pharmacother*. 2024;15(2):93–104.  
doi: 10.1177/0976500X241240634
21. Kanabar PN, Los NS, Lawal TO, Patel S, Raut NA, Maienschein-Cline M, *et al.* Combinations of vitamin A and D induced are synergistic in breast cancer cells and alter gene expression in the endoplasmic reticulum stress, unfolded protein and oestrogen signalling canonical. *Funct Foods Health Dis*. 2023;13(3):135–155.  
doi: 10.31989/ffhd.v13i3.1069
22. Ostos Mendoza KC, Garay Buenrostro KD, Kanabar PN, *et al.* Peonidin-3-O-glucoside and resveratrol increase the viability of cultured human hFOB osteoblasts and alter the expression of genes associated with apoptosis, osteoblast differentiation and osteoclastogenesis. *Nutrients*. 2023;15(14):3233.  
doi: 10.3390/nu15143233
23. Dobin A, Davis CA, Schlesinger F, *et al.* STAR: ultrafast universal RNA-seq aligner. *Bioinformatics*. 2013;29(1): 15–21.  
doi: 10.1093/bioinformatics/bts635
24. Liao Y, Smyth GK, Shi W. FeatureCounts: An efficient general-purpose program for assigning sequence reads to genomic features. *Bioinformatics*. 2014;30(7):923–930.  
doi: 10.1093/bioinformatics/btt656
25. McCarthy DJ, Chen Y, Smyth GK. Differential expression analysis of multifactor RNA-Seq experiments with respect to biological variation. *Nucleic Acids Res*. 2012;40(10):4288–4297.  
doi: 10.1093/nar/gks042
26. Benjamini Y, Hochberg Y. Controlling the false discovery rate: A practical and powerful approach to multiple testing. *J R Stat Soc Ser B (Methodol.)*. 1995;57(1):289–300.  
doi: 10.1111/j.2517-6161.1995.tb02031.x
27. Cai Y, Dai F, Ye Y, Qian J. The global burden of breast cancer among women of reproductive age: a comprehensive analysis. *Sci Rep*. 2025;15(1):9347.  
doi: 10.1038/s41598-025-93883-9
28. Sung H, Ferlay J, Siegel RL, Laversanne M, Soerjomataram I, Jemal A, Bray F. Global cancer statistics 2020: GLOBOCAN estimates of incidence and mortality worldwide for 36 cancers in 185 countries. *CA Cancer J Clin*. 2021;71(3):209–249.  
doi: 10.3322/caac.21660
29. Rotimi SO, Rotimi OA, Salhia B. A review of cancer genetics and genomics studies in Africa. *Front Oncol*. 2021;10:606400.  
doi: 10.3389/fonc.2020.606400
30. Orlando G, Ferrante C, Zengin G, *et al.* Qualitative chemical characterization and multidirectional biological investigation of leaves and bark extracts of *Anogeissus leiocarpus* (DC.) Guill. & Perr. (Combretaceae). *Antioxidants*. 2019;8(9):343.

- doi: 10.3390/antiox8090343
31. Assunção PID, da Conceição ED, Borges LL, Marciano de Paula JA. Development and validation of a HPLC-UV method for the evaluation of ellagic acid in liquid extracts of *Eugenia uniflora* L. (Myrtaceae) leaves and its ultrasound-assisted extraction optimization. *Evid Based Complement Alt Med*. 2017;2017(1):1501038.  
doi: 10.1155/2017/1501038
32. Cheng H, Lu C, Tang R, Pan Y, Bao S, Qiu Y, Xie M. Ellagic acid inhibits the proliferation of human pancreatic carcinoma PANC-1 cells in vitro and in vivo. *Oncotarget*. 2017;8(7):12301-12310.  
doi: 10.18632/oncotarget.14811
33. Wang F, Chen J, Xiang D, Lian X, Wu C, Quan J. Ellagic acid inhibits cell proliferation, migration, and invasion in melanoma via EGFR pathway. *Am J Transl Res*. 2020;12(5):2295-2304.
34. Naiki-Ito A, Chewonarin T, Tang M, et al. Ellagic acid, a component of pomegranate fruit juice, suppresses androgen-dependent prostate carcinogenesis via induction of apoptosis. *Prostate*. 2015;75(2):151-160.  
doi: 10.1002/pros.22900
35. Li TM, Chen GW, Su CC, et al. Ellagic acid induced p53/p21 expression, G1 arrest and apoptosis in human bladder cancer T24 cells. *Anticancer Res*. 2005;25(2A):971-979.
36. Kim H, Lee RA, Moon BI, Choe KJ. Ellagic acid shows different anti-proliferative effects between the MDA-MB-231 and MCF-7 human breast cancer cell lines. *J Breast Cancer*. 2009;12(2):85-91.  
doi: 10.4048/jbc.2009.12.2.85
37. Saleem A, Husheem M, Härkönen P, Pihlaja K. Inhibition of cancer cell growth by crude extract and the phenolics of *Terminalia chebula* retz. fruit. *J Ethnopharmacol*. 2002;81(3):327-336.  
doi: 10.1016/s0378-8741(02)00099-5
38. Golmohammadi M, Zamanian MY, Jalal SM, et al. A comprehensive review on ellagic acid in breast cancer treatment: From cellular effects to molecular mechanisms of action. *Food Sci Nutr*. 2023;11(12):7458-7468.  
doi: 10.1002/fsn3.3699
39. Chen HS, Bai MH, Zhang T, Li GD, Liu M. Ellagic acid induces cell cycle arrest and apoptosis through TGF- $\beta$ /Smad3 signaling pathway in human breast cancer MCF-7 cells. *Int J Oncol*. 2015;46(4):1730-1738.  
doi: 10.3892/ijo.2015.2870
40. Yousuf M, Shamsi A, Khan P, et al. Ellagic acid controls cell proliferation and induces apoptosis in breast cancer cells via inhibition of cyclin-dependent kinase 6. *Int J Mol Sci*. 2020;21(10):3526.  
doi: 10.3390/ijms21103526
41. Yousuf M, Shamsi A, Mohammad T, et al. Inhibiting cyclin-dependent kinase 6 by taurine: Implications in anticancer therapeutics. *ACS Omega*. 2022;7(29):25844-25852.  
doi: 10.1021/acsomega.2c03479
42. Wang N, Wang ZY, Mo SL, et al. Ellagic acid, a phenolic compound, exerts anti-angiogenesis effects via VEGFR-2 signaling pathway in breast cancer. *Breast Cancer Res Treat*. 2012;134(3):943-955.  
doi: 10.1007/s10549-012-1977-9
43. Papoutsis Z, Kassi E, Tsiapara A, Fokialakis N, Chrousos GP, Moutsatsou P. Evaluation of estrogenic/antiestrogenic activity of ellagic acid via the estrogen receptor subtypes ER $\alpha$  and ER $\beta$ . *J Agric Food Chem*. 2005;53(20):7715-7720.  
doi: 10.1021/jf0510539
44. Poirier D, Roy J, Maltais R. A targeted-covalent inhibitor of 17 $\beta$ -HSD1 blocks two estrogen-biosynthesis pathways: In vitro (metabolism) and in vivo (xenograft) studies in T-47D breast cancer models. *Cancers*. 2021;13(8):1841.  
doi: 10.3390/cancers13081841
45. Wang XQ, Aka JA, Li T, Xu D, Doillon CJ, Lin SX. Inhibition of 17 $\beta$ -hydroxysteroid dehydrogenase type 7 modulates breast cancer protein profile and enhances apoptosis by down-regulating GRP78. *J Steroid Biochem Mol Biol*. 2017;172:188-197.  
doi: 10.1016/j.jsbmb.2017.06.009
46. He W, Gauri M, Li T, Wang R, Lin SX. Current knowledge of the multifunctional 17 $\beta$ -hydroxysteroid dehydrogenase type 1 (HSD17B1). *Gene*. 2016;588(1):54-61.  
doi: 10.1016/j.gene.2016.04.031
47. Zhang CY, Wang WQ, Chen J, Lin SX. Reductive 17 $\beta$ -hydroxysteroid dehydrogenases which synthesize estradiol and inactivate dihydrotestosterone constitute major and concerted players in ER+ breast cancer cells. *J Steroid Biochem Mol Biol*. 2015;150:24-34.  
doi: 10.1016/j.jsbmb.2014.09.017
48. Kang Y, Massagué J. Epithelial-mesenchymal transitions: twist in development and metastasis. *Cell*. 2004;118(3):277-279.  
doi: 10.1016/j.cell.2004.07.011
49. Wang Y, Liu J, Ying X, Lin PC, Zhou BP. Twist-mediated epithelial-mesenchymal transition promotes breast tumor cell invasion via inhibition of Hippo pathway. *Sci Rep*. 2016;6:24606.  
doi: 10.1038/srep24606
50. Wu S, Du Y, Beckford J, Alachkar H. Upregulation of the EMT marker vimentin is associated with poor clinical outcome in acute myeloid leukemia. *J Transl Med*. 2018;16(1):170.

doi: 10.1186/s12967-018-1539-y

51. Berr AL, Wiese K, Dos Santos G, *et al.* Vimentin is required for tumor progression and metastasis in a mouse model of non-small cell lung cancer. *Oncogene*. 2023;42(25):2074-2087.

doi: 10.1038/s41388-023-02703-9

52. Usman S, Waseem NH, Nguyen, TKN, *et al.* Vimentin is at the heart of epithelial mesenchymal transition (EMT) mediated metastasis. *Cancers*. 2021;13:4985.

doi: 10.3390/cancers13194985.

53. Du W, Liu X, Yang M, Wang W, Sun J. The regulatory role of PRRX1 in cancer epithelial-mesenchymal transition. *Onco*

*Targets Ther*. 2021;14:4223-4229.

doi: 10.2147/OTT.S316102.

54. Pandey P, Khan F, Upadhyay TK, Seungjoon M, Park MN, Kim B. New insights about the PDGF/PDGFR signalling pathway as a promising target to develop cancer therapeutic strategies. *Biomed Pharmacother*. 2023;161:114491.

doi: 10.1016/j.biopha.2023.114491.

55. Lim SC, Hwang H, Han SI. Ellagic acid inhibits extracellular acidity-induced invasiveness and expression of COX, Snail, Twist 1, and c-myc in gastric carcinoma cells. *Nutrients*. 2019;11(12):3023-3034.

doi: 10.3390/nu11123023.

# Appendix

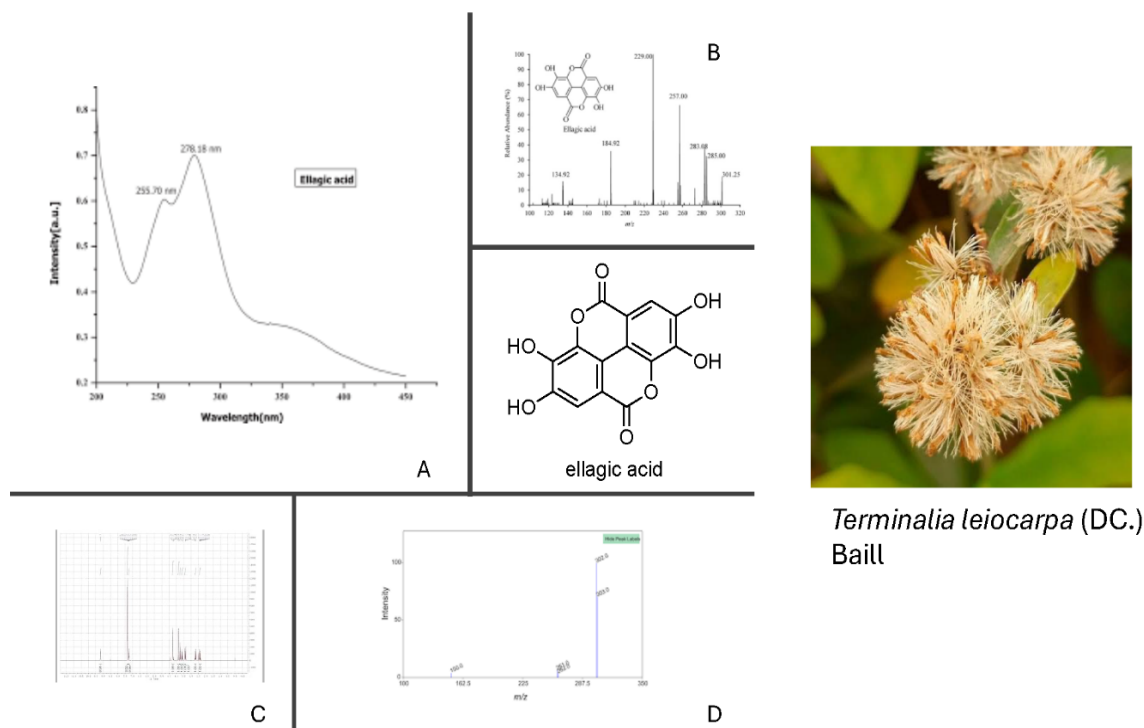


**Figure A1.** Isolation and characterization of ellagic acid from *Terminalia leioarpa* (DC.) Baill. [syn. *Anogeissus leioarpus* DC (Combretaceae)]. Ellagic acid from *Terminalia leioarpa* (DC.) Baill. [syn. *Anogeissus leioarpus* DC (Combretaceae)] was identified unambiguously using (A) ultraviolet spectroscopy, (B) mass spectrometry, and (C) <sup>1</sup>H and (D) <sup>13</sup>C nuclear magnetic resonance spectra. All experimental data agreed with the literature data.

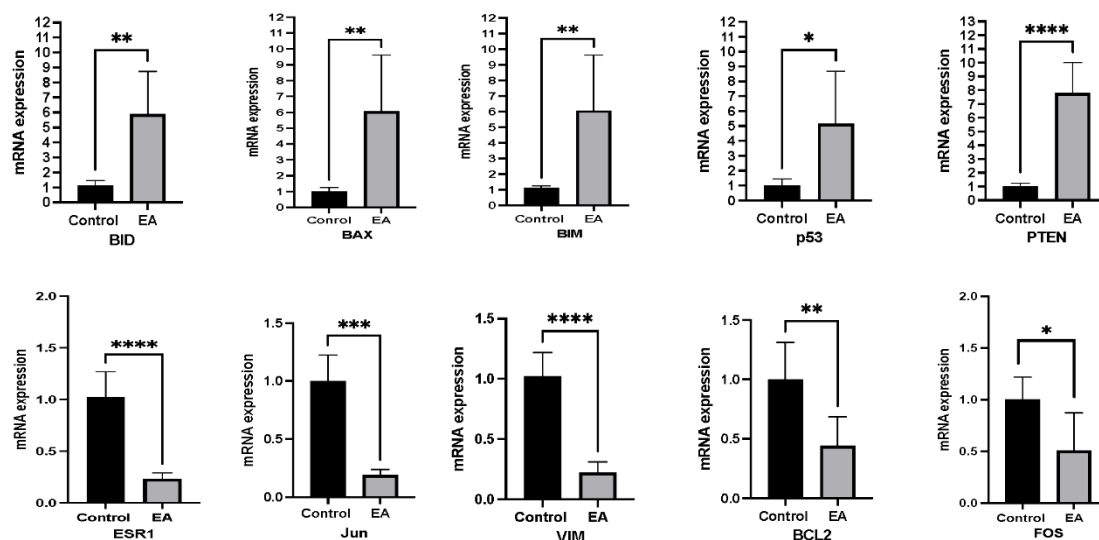


**Figure A2.** Quantitative polymerase chain reaction validation of targeted gene expression from RNA isolated from ellagic acid (EA)-treated human MCF-7 breast cancer cells versus control MCF-7 cells (0.01% dimethyl sulfoxide). (A) EA treatment of MCF-7 cells upregulated the expression of genes in the B cell lymphoma 2 family of pro-apoptotic proteins, namely *BID* (5.8 fold;  $p \leq 0.01$ ), *BAX* (>6 fold;  $p \leq 0.01$ ), *BIM* (>5.5 fold;  $p \leq 0.01$ ), and genes for the tumor suppressors *p53* (>4.8 fold;  $p \leq 0.05$ ) and *PTEN* (>7 fold;  $p \leq 0.0001$ ). (B) EA treatment of MCF-7 cells downregulated the expression of *ESR1* ( $p \leq 0.0001$ ), *JUN* ( $p \leq 0.001$ ), *VIM* ( $p \leq 0.0001$ ), *BCL2* ( $p \leq 0.01$ ), and *FOS* ( $p \leq 0.05$ ) as compared with control. Gene expression was quantified using  $\beta$ -actin as the gene with the  $\Delta\Delta$ CT method. Statistical analyses were performed using a Student *t*-test in GraphPad v10.6, with \*  $p \leq 0.05$ , \*\*  $p \leq 0.01$ , \*\*\*  $p \leq 0.001$ , \*\*\*\*  $p \leq 0.0001$ .